Vibration monitoring instrumentation system for detecting airgap eccentricity in mine winder motor

Capital investment in the underground coal mines is increasing day by day, than any other industry, therefore coal production has to be very efficient to make commercially viable. In this condition the economics of production would primarily depend on machine utilization indicated by machine availability, hence machine available time should be maximized, for best returns on capital invested and utilization of power.

This paper describes vibration monitoring instrumentation system for online monitoring of eccentricity in mine winder motor. The motor vibration is being sensed with the help of aaccelerometer and the vibration signal is conditioned using signal conditioners like low pass filter, high pass filter and band pass filter. Airgap eccentricity in the mine winder will produce unbalance magnetic pull (UMP) in the mine winder motor.

A novel condition monitoring instrumentation system based on motor vibration component has been developed for online condition monitoring of mine winder motor. The instrumentation system is able to diagnose the airgap eccentricity of mine winder motor, which increase the safety as well as availability of mine winder.

Keywords: *Condition monitoring, mine winder motor, motor vibration, state variable band pass filter.*

Introduction

Mine winder is driven by 3 phase slip-ring induction motor. Failure of mine winder motor during operation will cause for loss of coal production along with safety of personnel. Hence, it would be beneficial to have online condition monitoring for such motor to detect incipient fault and enable planned preventive maintenance or repair. For many years, planned maintenance strategies have been used in coal mines to ensure failure of mine winder motor is minimum.

Bearing failure might manifest themselves as rotor asymmetry faults [2], which are usually covered under the category of eccentricity related faults, or bearing failure can be categorized as [1] outer bearing race defect, inner bearing defect ball defect and train defect.

The majority of the electrical machines use ball bearings. Each bearing consists of two rings-one inner and the other outer. A set of balls or rolling elements placed in raceways rotates inside these rings [2]. Even under normal operating conditions with balanced load and good alignment, fatigue failures may take place. These faults may lead to increased vibration and noise levels. Flaking or spalling of bearings might occur when fatigue causes small pieces to break loose from the bearing.

Other than the normal internal operating stresses caused by vibration, inherent eccentricity, and bearing currents [3] due to solid state drives, bearings can be spoiled by many other external causes such as the following:

1. Contamination and corrosion caused by pitting and sanding action of hard and abrasive minute particles or corrosive action of water, acid, etc.;
2. Improper lubrication, which includes both over and under lubrication causing heating and abrasion;
3. Improper installation of bearing, by improperly forcing the bearing onto the shaft or in the housing (due to misalignment), indentations are formed in the raceways (brinelling).

The paper reports on a study carried out to detect airgap eccentricity due to bearing failure using non-invasive traducers to monitor the motor vibration. The theoretical predictions have been verified by experimental test results i.e. online vibration monitoring instrumentation system.

Previous research on airgap eccentricity in large induction motor

Airgap eccentricity and unbalanced magnetic pull (UMP) have been researched since the beginning of this century; hence there is an abundance of published literature on the subject. Many of the classical papers have concentrated on the calculation of the airgap field as a function of eccentricity [3] and others have identified the principal factors causing UMP [4]. The design of rotor assemblies, critical speeds, slot combinations, windings, vibration problems and the calculation of vibratory forces and acoustic noise have all

Mr. Ananda Shankar Hati, Indian School of Mines, Dhanbad, India. aryan1437@gmail.com; hati.a.mme@ismdhanbad.ac.in

been researched in relation to airgap eccentricity and UMP [5-13]. However, the research has not been directed to the development of online diagnostics, but it could be argued that parameters were identified which were certainly functions of airgap eccentricity and UMP and that this should suffice for the development of an online monitor.

ECCENTRICITY

Airgap eccentricity can occur in the form of static or dynamic eccentricity. In the case of static eccentricity, the position of minimum radial airgap length is fixed in space. For example, static eccentricity can be caused by stator core ovality or incorrect positioning of the rotor or stator at the commissioning stage. Provided that the rotor-shaft assembly is sufficiently stiff, then the level of static eccentricity should not change. Dynamic eccentricity occurs when the centre of the rotor is not at the centre of rotation and the minimum airgap revolves with the rotor. This means that dynamic eccentricity is a function of space and time. Dynamic eccentricity could be caused by a bent shaft, mechanical resonances at critical speeds, or bearing wear and movement. It is also possible that high levels of static eccentricity can produce unacceptable levels of UMP which can result in shaft flexing and dynamic eccentricity thus increasing the risk of a rub between the rotor and stator.

AIRGAP FLUX DISTRIBUTION

The analysis is based on the rotating wave approach whereby the magnetic flux waves in the airgap are taken as the product of permeance and magnetomotive force (MMF) waves (20).

This means that the airgap field is complex and comprises the following components:

(a) Fundamental
(b) Stator and rotor MMF harmonics
(c) Stator and rotor slot permeance harmonics
(d) Airgap eccentricity permeance harmonics
(e) Permeance harmonics due to saturation

In the following analysis, the specific permeance Λ is termed as the permeance.

The permeance of an airgap bounded by a slotted stator and a smooth rotor is given by

... (1)

where,

Λ = specific permeance

st = stator,

θ = space variable, rad

n = any integer

S = number of stator slots

The permeance of an airgap bounded by a slotted rotor and a smooth rotor is given by

$$\Lambda_{rt}(\theta,t) = \sum_{n_{rt}=0}^{\infty} \Lambda n_{rt} \cos\{n_{rt} R(\theta - \omega_r t)\} \qquad \text{... ...} \quad (2)$$

where,

rt = rotor

t = time variable, s

R = number of rotor slots

ω_r = rotational speed, rad/s

The resultant of these permeances can be expressed as the product of a constant and the values of the two permeances

$$\Lambda_{rt,st}(\theta,t) = \sum_{n_{rt}=0}^{\infty} \sum_{n_{st}=0}^{\infty} \Lambda n_{rt}, n_{st} \cos \times$$

$$\{(n_{rt} R \pm n_{st} S)\theta - n_{rt} R \omega_r t\} \qquad \text{... ...} \quad (3)$$

In the presence of static eccentricity, the radial airgap length is a function of space only. Assuming a smooth stator and rotor the permeance will be

$$\Lambda_{se}(\theta) = \sum_{n_s=0}^{\infty} \Lambda n_s \cos n_s \theta \qquad \text{... ...} \quad (4)$$

where,

s, se = static

$$\left(\Phi/s,\right) Wb/ \quad \Lambda_{st}(\theta) = \sum_{n_{st}=0}^{\infty} \Lambda n_{st}^2 \cos n_{st} S\theta$$

The magnitude of the harmonic permeance waver due to static eccentricity are found by Fourier analysis to be

$$\Lambda n_s = \frac{\mu_0}{g'} \frac{\left\{1 - \sqrt{1 - (\varepsilon')^2}\right\}^{n_s}}{(\varepsilon')^{n_s} 1 - (\varepsilon')^2} \qquad \text{... ...} \quad (5)$$

where,

n_s = 1,2,3...

μ_0 = permeability of free space, H/m

g' = effective mean airgap length in the presence of sloting, m

ε' = effective relative eccentricity = e/g'

Eqn. (5) shows that as the level of static eccentricity increases, the magnitude of Λn_s will also increase.

The radial airgap length in the presence of dynamic eccentricity is a function of space and time. The permeance can thus be represented as

$$\Lambda_{de}(\theta,t) = \sum_{n_d=0}^{\infty} \Lambda n_d \cos\{n_d(\theta - \omega_r t)\} \qquad \text{... ...} \quad (6)$$

where

d, de = dynamic

Saturation can be represented by a permeance wave with twice the number of poles and twice the frequency of the fundamental wave [24] because the airgap becomes effectively larger in the regions of maximum flux density. Hence, the permeance of smooth and concentric airgap combined with the effects of saturation is expressed as

$$\Lambda_{sa}(\theta,t)=\sum_{n_{sa}=0}^{\infty}\Lambda n_{sa}\cos\{n_{sa}(2p\theta-2\omega_1 t)\} \quad \text{... ...} \quad (7)$$

where,

sa = saturation

p = number of pole pairs

ω_1 = angular supply frequency, rad/s

Combining eqn. 3, 4, 6 and 7 in the way in which the permeance due to slotting were combined gives the total permeance as

$$A_{tot}(\theta,t)=$$

$$\sum_{n_{rt}=0}^{\infty}\sum_{n_{st}=0}^{\infty}\sum_{n_s=0}^{\infty}\sum_{n_d=0}^{\infty}\sum_{n_{sa}=0}^{\infty}\times\Lambda n_{rt},n_{st},n_s,n_d,n_{sa}$$

$$\times\cos\{(n_{rt}R\pm n_{st}S\pm n_s\pm n_d\pm 2n_{sa}p)\theta$$

$$-((n_{rt}R\pm n_d)\omega_r\pm 2n_{sa}\omega_1)t\} \quad \text{... ...} \quad (8)$$

The magnetomotive force produced by the current flowing in the stator and rotor windings consists of a series of space and time harmonics. This can be represented by (neglecting phase angle and skew)

$$F_{tot}(\theta,t)=\sum_{n_{\theta s}=0}^{\infty}\sum_{n_{\omega s}=0}^{\infty}Fn_{\theta s},n_{\omega s}\cos(n_{\theta s}p\theta-n_{\omega s}\omega_t t)+$$

$$\sum_{n_{\theta r}=1}^{\infty}\sum_{n_{\omega r}=-\infty}^{\infty}Fn_{\theta r},n_{\omega r}\times\cos\{n_{\theta r}p\theta-(n_{\omega r}s\omega_t+n_{\theta r}p\omega_r)t\}$$

$$\text{... ...} \quad (9)$$

where,

s = per unit slip

ωr = rotor time harmonic

The flux density distribution in the airgap is given as the product of the permeance and the MMF. Combining equation 8 and 9 gives the resulting expression as:

$$B(\theta,t)=\sum_{m_s,\Omega_s}Bm_s,\Omega_s\cos(m_s\theta-\Omega_s t)+$$

$$\sum_{m_r,\Omega_r}Bm_r,\Omega_r\cos(m_r\theta-\Omega_r t) \quad \text{... ...} \quad (10)$$

where,

B = flux density, T

$$m_s=n_{rt}R\pm n_{st}S\pm n_s\pm n_d\pm 2n_{sa}p\pm n_{\theta s}p$$

$$\Omega_s=(n_{rt}R\pm n_d)\omega_r\pm 2n_{sa}\omega_1\pm n_{\omega s}\omega_1$$

$$m_r=n_{rt}R\pm n_{st}S\pm n_s\pm n_d\pm 2n_{sa}p\pm n_{\theta r}p$$

$$\Omega_r=(n_{rt}R\pm n_d\pm n_{\theta r}p)\omega_r\pm 2n_{sa}\omega_1\pm n_{\omega r}s\omega_1$$

The flux density distribution varies in both space and time and the time component gives expressions for predicting the frequency content of the flux density waveform. These expressions are expressed as follows:

$$f_{sh^1}=\left\{(n_{rt}R\pm n_d)\frac{(1-s)}{p}\pm 2n_{sa}\pm n_{\omega s}\right\}f_1 \quad \text{... ...} \quad (11)$$

$$f_{sh^2}=\left\{(n_{rt}R\pm n_d\pm n_{\theta r}p)\frac{(1-s)}{p}\pm 2n_{sa}\pm n_{\omega r}s\right\}f_1 \quad \text{...} \quad (12)$$

where,

f_{sh} = frequency of flux density or current slot harmonic, Hz

ωs = stator time harmonic

θr = rotor space harmonic

As these harmonics fluxes are moving relative to the stator, they should induce corresponding current harmonics in the stationary stator winding. Hence, it should be possible to detect airgap eccentricity by analyzing the stator current spectrum.

Vibration harmonics for airgap eccentricity of motor

The radial force waves acting on the stator core structureare proportional to the square of the flux density waveform [25]. In terms of the force per unit area, the force wave distribution can be determined from:

$$\sigma(\theta,t)=\frac{B^2(\theta,t)}{2\mu_0} \quad \text{... ...} \quad (13)$$

Substituting eqn 10 into eqn 13 gives:

$$\sigma(\theta,t)=\sum_{m\Omega}\sigma m,\Omega\cos(m\theta-\Omega t) \quad \text{... ...} \quad (14)$$

where,

$$m=n'_{rt}R\pm n'_s S\pm n'_s\pm n'_d\pm 2n'_{sa}p\pm n'_\theta p$$

$$\Omega=(n'_{rt}R\pm n'_d)\omega_r\pm 2n'_{sa}\omega_1\pm n'_\omega\omega_1$$

The time component of this expression gives an equation for predicting the harmonic content of the vibration forcing function and is expressed as:

$$f_{sv}=\left\{(n'_{rt}R\pm n'_d)\frac{(1-s)}{p}\pm 2n'_{sa}\pm n'_\omega\right\}f_1 \quad \text{... ...} \quad (15)$$

These harmonic forces acting on the core will cause vibration of the same frequency to be transmitted to the surface of the stator core. Hence the surface vibration signal will contain frequency components characteristic of static and dynamic eccentricity.

A preliminary study by Thomson et al. [26] has shown that one of the principal slot harmonics in the stator frame vibration changed as a function of static eccentricity. It was observed that the change in the monitored parameter was a function of the transducer position around the periphery of the frame.

VIBRATION SLOT HARMONICS

In general eqn no. 15 can be used to predict the frequency content of vibration signal

$$de_1 = \left\{ \left(n'_{rt}\ R - n'_d \right) \frac{(1-s)}{p} + 2n'_{sa} + n'_{\omega} \right\} f_1 \quad \ldots\ldots \quad (16)$$

where, de_1 = dynamic eccentricity component –

$1;\ n'_{rt} = 1;\ R = 28;\ n'_d = 1;\ s = 0.02;\ p = 2;\ n'_{sa} = 1;$

$n'_{\omega} = 2;\ f_1 = 50Hz$

de = 861.5 Hz

$$psh = \left\{ \left(n'_{rt}\ R - n'_d \right) \frac{(1-s)}{p} + 2n'_{sa} + n'_{\omega} \right\} f_1 \quad \ldots\ldots \quad (17)$$

where, psh = principal slot harmonics;

$n'_{rt} = 1;\ R = 28;\ n'_d = 0;\ s = 0.02;\ p = 2;\ n'_{sa} = 0;$

$n'_{\omega} = 2;\ f_1 = 50Hz$

psh = 886 Hz

$$de_2 = \left\{ \left(n'_{rt}\ R + n'_d \right) \frac{(1-s)}{p} + 2n'_{sa} + n'_{\omega} \right\} f_1 \quad \ldots\ldots \quad (18)$$

where, de_2 = dynamic eccentricity component –

$2;\ n'_{rt} = 1;\ R = 28;\ n'_d = 1;\ s = 0.02;\ p = 2;\ n'_{sa} = 0;$

$n'_{\omega} = 2;\ f_1 = 50Hz$

de = 910.5 Hz

The predicted vibration harmonics for model winder motor of rating10 kW, 440 volt, 50 Hz, 4 pole, 3-phase slip-ring induction motor with 28 number of rotor slot and full load slip of 2% are 886 Hz (i.e. principal slot harmonics), 861.5 Hz (i.e. lower sideband harmonics) and 910.5 Hz (i.e. upper sideband harmonics).

The state variable bandpass filters of centre frequencies 886 Hz, 861.5 Hz and 910.Hz have been designed. The design of 861.5 Hz state variable bandpass filter is shown below.

Design of 861.5 Hz. filter

DESIGN REQUIREMENTS

f_o = 861.5 Hz.

Q = 50

Device data (ΔT = -55 to +125°C and ±12 V supply voltages)

$\Delta R/R$ = +0.018 (all resistors)

$\Delta C/C$ = -0.027 (all capacitors)

I_b = 0.5 µA (max.)

Nominal values of R_8 and R_9 are

$$10^8/f_o = 10^8/861.5 = 1.2\times10^5\,\Omega$$

Nominal values of C_1 and C_2 are

$$10^7/f_o = 10^7/861.5 = 1.2\times10^{-10}\,F$$

Nominal values of R_7 and R_{14} are

$$1/2\pi f_o C_1 = 1/2\pi(861.5)\times\left(1.2\times10^{-10}\right) = 1.5\times10^6\,\Omega \quad .$$

These resistors will cause an output offset voltage in IC2 and IC3of $I_bR_7 = 0.5\times10^{-6}\times1.5\times10^6 = 0.8$ V. To prevent this offset at output of IC2 and IC3, we will use two of the circuits shown in the fig.

$$R_7 = R_{14} = \frac{10^{10}}{R_7 - 2\times10^5} = \frac{10^{10}}{1.5\times10^6 - 2\times10^5}$$

$$= 7.7\times10^3\,\Omega$$

As an additional guard against offsets we can return the non-inverting inputs of IC2 and IC3 to ground through 100kΩ + 7.14 kΩ = 107.14 kΩ.

We set $R_1 = R_8 = 1.2\times10^5\Omega$.

R_4 is found from

$R_4 = R_1(2Q-1) = 1.1\times10^5\ (2\times50-1) = 1.2\times10^7\Omega$.

This value of R_4 appears to be impractical. We can use the same tee recommended above to solve this problem. The required value of R_4 is

$$R_4 = \frac{10^{10}}{1.2\times10^7 - 2\times10^5} = 8.5\times10^2\,\Omega \quad .$$

The circuit gain H at resonance is

$$H = R_4/R_1 = 1.2\times10^7/1.2\times10^5 = 99\,.$$

Sensitivity-function computations for f_o variations are as follows:

RESISTORS

$$S^{f_o}_{R_8} = \frac{1}{2}$$

$$S^{f_o}_{R_9} = S^{f_o}_{R_7} = S^{f_o}_{R_{14}} = -\frac{1}{2}$$

The $\Delta R/R$ = +0.018 (-55 to + 125°C) specified for all resistors will cause f_o to increase by $1/2(0.018)861.5Hz. = 7.8Hz.$ owing to R_8. Resistors R_9, R_7 and R_{14} will each cause f_o to decrease by the same amount.

CAPACITORS

$$S^{f_o}_{C_1} = S^{f_o}_{C_2} = -\frac{1}{2}$$

The $\Delta C/C = -0.027$ specified for each capacitor will cause f_o to increase by $-1/2(-0.027)861.5Hz. = 11.6Hz.$

The total shift in f_o due to parameter variations of the above six components will be + 7.8 - 7.8 - 7.8 - 7.8 + 11.6 +

11.6 = + 7.6 Hz. This 7.6 per cent positive frequency shift will occur as the temperature increases from -55 to +125°C.

Sensitivity-function computations for Q variations are as follows:

RESISTORS R_1 AND R_4

$$S^{f_o}_{R_1} = S^{f_o}_{R_4} = \frac{R_2}{R_1 + R_4} = \frac{1.39\times10^7}{\left(1.4\times10^5\right)+\left(1.39\times10^7\right)} = 0.99$$

This will cause Q to vary by 0.99(0.018)711.5 = 12.7 as the temperature varies from -55 to +125°C.

RESISTORS R_8 AND R_9

$$S^{f_o}_{R_8} = S^{f_o}_{R_9} = \frac{1}{2} - \frac{R_3}{R_8 + R_9}$$

$$= \frac{1}{2} - \frac{1.4\times10^5}{\left(1.4\times10^5\right)+\left(1.4\times10^5\right)} = 0$$

RESISTORS R_7 AND R_{14}

$$S^{f_o}_{R_7} = S^{f_o}_{R_{14}} = \frac{1}{2}$$

The change in Q due to this sensitivity function is $\frac{1}{2}(0.018)711.5 = 6.4$

CAPACITORS

$$S^{f_o}_{C_1} = S^{f_o}_{C_2} = \frac{1}{2}$$

TABLE 1: TABLE SHOWS THE FILTER CIRCUIT PARAMETERS IN STATE VARIABLE BANDPASS FILTERS OF CENTER FREQUENCY 861.5 Hz, 886 Hz AND 910.5 Hz

Filter circuit parameters	Filter circuit parameters at specified center frequency of state variable bandpass filter		
	861.5 Hz	886 Hz	910.5 Hz
R_1	1.2×10^5 Ω	1.1×10^5 Ω	1.1×10^5 Ω
R_2	100 kΩ	100 kΩ	100 kΩ
R_3	100 kΩ	100 kΩ	100 kΩ
R_4	8.5×10^2 Ω	9.3×10^2 Ω	8.5×10^2 Ω
R_6	100 kΩ	100 kΩ	100 kΩ
R_6	100 kΩ	100 kΩ	100 kΩ
R_7	7.7×10^3 Ω	7.1×10^3 Ω	7.1×10^3 Ω
R_8	1.2×10^5 Ω	1.1×10^5 Ω	1.1×10^5 Ω
R_9	1.2×10^5 Ω	1.1×10^5 Ω	1.1×10^5 Ω
R_{10}	100 kΩ	100 kΩ	100 kΩ
R_{11}	7.14 kΩ	7.14 kΩ	7.14 kΩ
R_{12}	100 kΩ	100 kΩ	100 kΩ
R_{13}	100 kΩ	100 kΩ	100 kΩ
R_{14}	7.7×10^3 Ω	7.1×10^3 Ω	7.1×10^3 Ω
R_{15}	100 kΩ	100 kΩ	100 kΩ
R_{16}	7.14 kΩ	7.14 kΩ	7.14 kΩ
C_1	1.2×10^{-10} F	1.1×10^{-10} F	1.1×10^{-10} F
C_2	1.2×10^{-10} F	1.1×10^{-10} F	1.1×10^{-10} F

The change in Q due to changes in each capacitance is $\frac{1}{2}(-0.027)711.5 = -9.61$.

The total change in Q as the temperature varies from -55 to +125°C will be 12.7 + 12.7 + 6.4 + 6.4 - 9.61 - 9.61 = 18.98

Percentage change is Q due to change in temperature is 18.98.

Fig.1 shows the circuit diagram of the state variable bandpass filters.

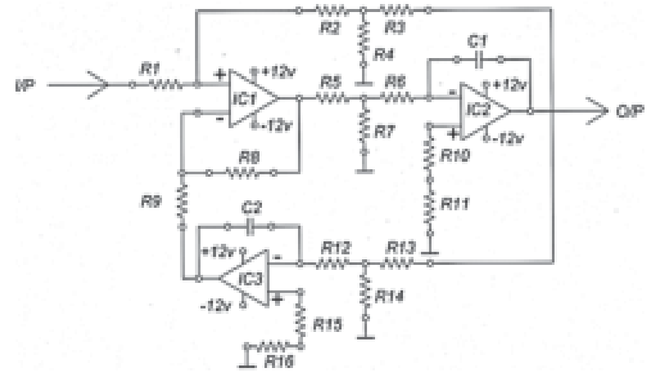

Fig.1 Circuit diagram of a state variable band pass filter

Fig.2 shows the output voltage of state variable bandpass filter of center frequency of 861.5 Hz at constant input voltage of variable frequency. The output voltage of state variable bandpass filter frequency is maximum at constant input voltage magnitude where the input voltage frequency become 861.5 Hz. Similarly 836 Hz and 910.5 Hz state variable bandpass filter have been designed. Table 1 shows the circuit parameters of state variable bandpass filter of 861.5 Hz, 886 Hz. and 910.5 Hz.

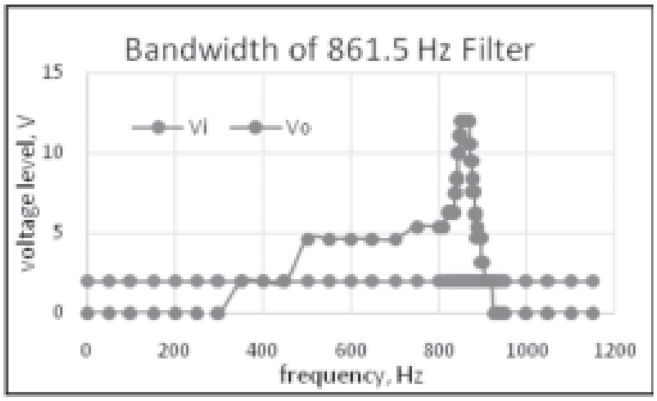

Fig.2 Bandwidth of 861.5 Hz filter

The developed instrumentation system

In laboratory for the purpose of fault simulation a10 kW, 440 volt, 50 Hz, 3-phase slip-ring induction motor to represent a winder motor is used. An online eccentricity monitoring instrumentation system for the model mine winder motor has been developed.Airgap eccentricity have been simulated in the laboratory to ascertain the effectiveness of the instrumentation system developed. Motor vibrationis being sensed using accelometers. The output of accelerometers are fed into signal conditioners which are a set of filters comprising low pass filter, high pass filter and a band pass filter. To isolate the principal slot harmonic and sidebands very accurately, the output of each signal conditioner is connected with three numbers of state variable band pass filter (SVBPF). The output of SVBPF are connected to LED bargraph meter for measuring the magnitude of principal slot harmonic and sidebands. Fig.3 shows the block diagram of the complete instrumentation system.

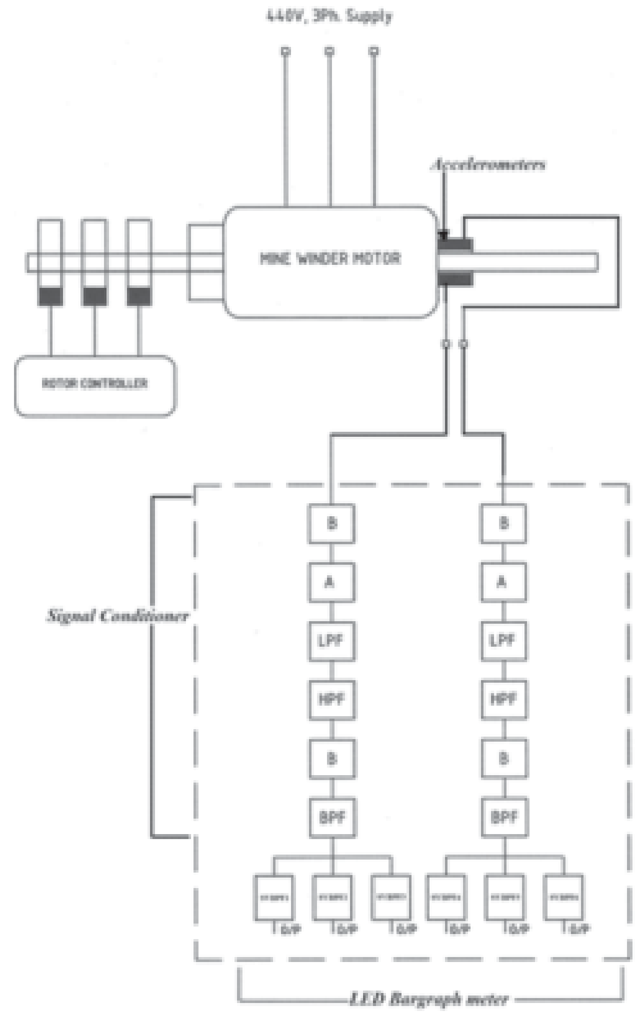

Fig.3 Block diagram of vibration monitoring instrumentation system

Experimental results

Figs.4A and 4B show the experimental set up having 10 kW M-G set with resistive load connected with the generator for loading of 3-phase slip ring induction motor. The 3-phase slip-ring induction motor represents the mine winder motor. The motor is designed and constructed for the simulation of stator and rotor winding faults which normally a winder motor encounters.

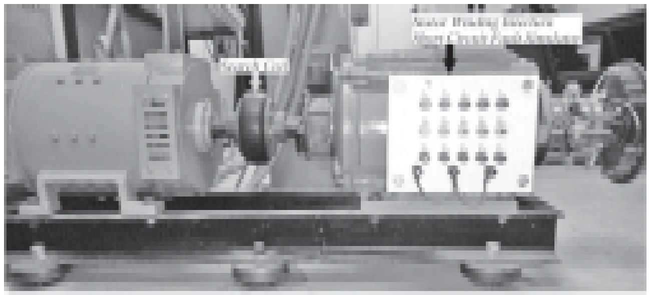

Fig.4A 10kW M-G set represents model mine winder motor with loading arrangement

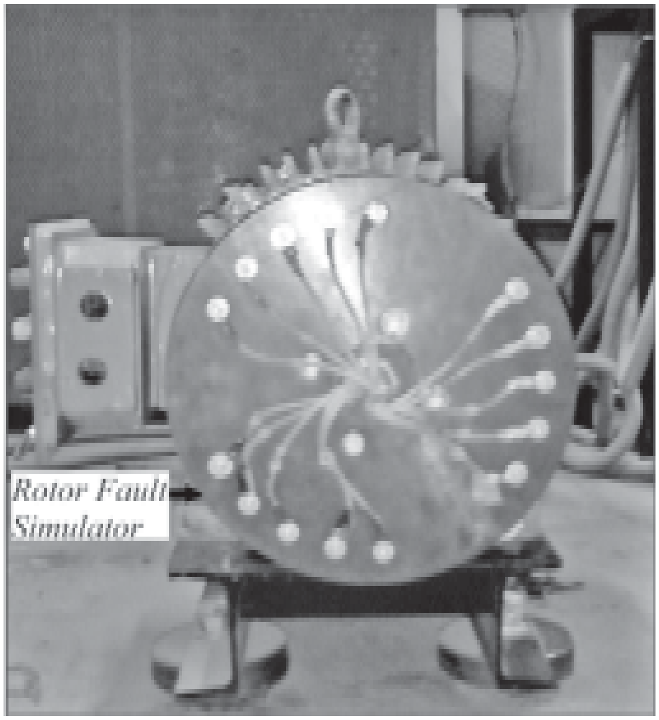

Fig.4B Photograph of mine winder motor fault simulator to simulate interturn short circuit fault of rotor winding

Fig.5 shows the complete circuit diagram of the online condition monitoring instrumentation system, developed in the research work for the diagnosis of winder motor faults.

Active first order low pass filters (LPFs) have been used along with active first order high pass filter (HPFs) and active first order band pass filter (BPFs) to obtain accurate band of frequencies that will be comprising of primary harmonics and sidebands.

Fault simulation details

Motor healthy

The 10 kW, 440 V, 50 Hz, 3-phase slip-ring induction motor under test was run under healthy condition for different loading conditions. The output of the 861.5 Hz filter and 910.5 Hz filter were found to be practically very low during these healthy run of the drive. Under different loading conditions of the drive, the output of the 886 Hz filter increased with

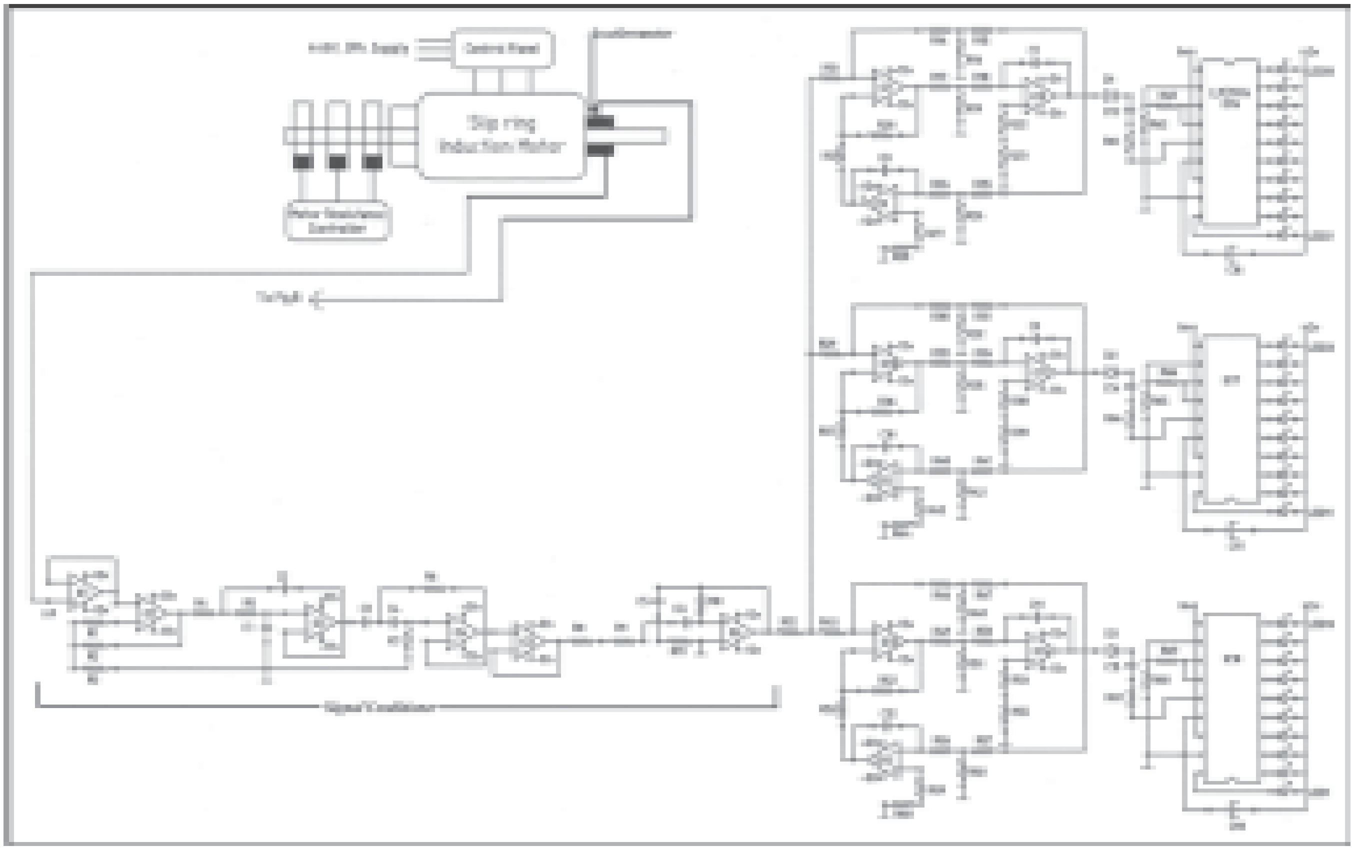

Fig.5 Circuit diagram of online condition monitoring instrumentation system for mine winder motor

increased loading condition.. The outputs of filters are shown in Fig.6. Ch. 1, Ch. 2 and Ch. 3 of Fig.6 shows the output voltage of 886 Hz. filter, 861.5 Hz filter and 910.5 Hz respectively during operation of motor.

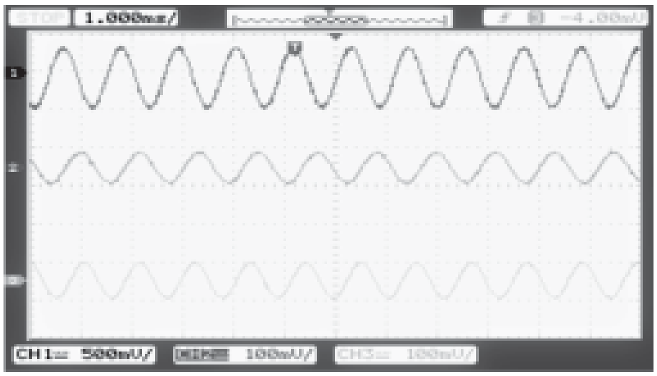

Fig.6 Upper trace show the output of 886 Hz filter, middle traceshow the output of861.5 Hz filter and lower traceshows the output 910.5 Hz

Eccentric running

Eccentric running of the motor may occur due to the bearing failure of the motor. During eccentric running of motor the output of principal slot harmonics i.e. 886 Hz. and sidebands i.e. 861.5 Hz. and 910.5 Hz increases. Fig.7 shows the output of the state variable filters at eccentric running.

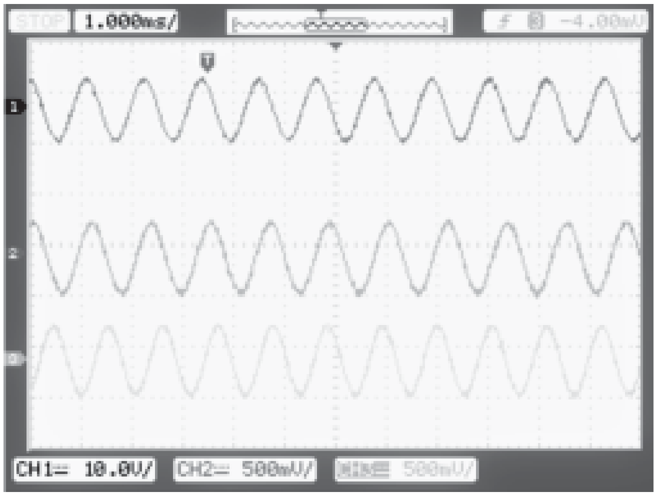

Fig.7 Upper trace show the output of 886 Hz filter, middle traceshow the output of 861.5 Hz filter and lower traceshows the output 910.5 Hz

Ch. 1, Ch. 2 and Ch. 3 of Fig.7 shows the output voltage of 886 Hz. filter, 861.5 Hz filter and 910.5 Hz respectively during eccentric running of the motor.

It has been observed that the magnitude of the sidebands at frequencies of 861.5 Hz and 910.5 Hz have considerably due to bearing failure or eccentric running of the rotor. The magnitude of principal slot harmonics has also increased

TABLE 2: STATE VARIABLE FILTER OUTPUT DURING VARIOUS CONDITION OF MOTOR

Motor condition	Frequency		
	886 Hz	861.5 Hz	910.5 Hz
Healthy	0.7 mV	100 mV	100 mV
Eccentric running	10 V	500 mV	500 mV

compared to healthy motor. Increase in the magnitude of sidebands and principal slot harmonics frequency indicates the condition of bearing failure. The output of principal slot harmonics and sidebands will be shown by the LED bargraph which will indicate the motor bearing condition.

Conclusion

Vibration monitoring based on line condition monitoring instrumentation system has been designed and developed for fault diagnosis of a model winder motor of rating 10 kW, 3 phase, 430 V, 50 Hz. slip ring induction motor. The model winder motor is designed and constructed to simulate various electrical faults which normally a mine winder motor encounters. The instrumentation system is very effective for fault diagnosis of the mine winder motor. The developed instrumentation system can be tailor made for a particular mine winder drive and can be used for on-line condition monitoring of mine winder drive. The same instrumentation system can be developed as a prototype hand held instrumentation system for the fault diagnosis of several other induction motors.

References

1. Von Kaehne, P. (1963): Unbalanced magnetic pull in electricalmachines. ERA Report Z/T142, ERA Technology Ltd., Leatherhead, Surrey, UK, 1963.
2. Rai, G. B. (1974): Airgap eccentricity in induction motors. ERA Report 741188, ERA Technology Ltd., Leatherhead, Surrey, UK, 1974.
3. Swann, S. A. (1963): "Effect of rotor eccentricity on the magnetic field inairgap of a nonsalient pole machine," Proc. IEE, 1963, 110, (5), pp.903-915.
4. Binns, K. J., and Dye, M. (1973): "Identification of principal factorscausing unbalanced magnetic pull in cage induction motors," Proc. IEE, 1973, 120, (3), pp. 349-354.
5. Crawford, W. G. (1951): "Unbalanced magnetic pull and the mechanicalstability of rotating electrical machines," *Eng.*, 1951, 171, pp. 504-505.
6. Bradford, M. (1968): "Unbalanced magnetic pull in a 6-pole inductionmoto," Proc. IEE, 1968, 115, (11), pp. 1619-1627.
7. Summers, E. W. (1955): "Vibration in 2-pole induction motors related toslip frequency," *Trans. Amer. Inst. Electr. Eng.*, 1955, pp. 69-72.
8. Kovacs, K. P. (1977): "Two-pole induction motor vibrations caused by homopolar alternating fluxes," *IEEE Trans.*, 1977, PAS-96, (4), pp. 1105-1108.
9. Freise, W. and Jordan, H. (1983): "Unilateral magnetic pull in 3-phase machines." CEGB CE-Trans 7836, 1983 from ETZ-A, 1962, 83, (9), pp. 299-303.
10. Jordan, H., Roder, G. and Weis, H. (1967): "Under what circumstances may mechanical vibrations of the stator core be expected at supply frequency in 4-pole, 3-phase asynchronous machines." ERA Translation IB 2578 from Elektrie, 1967, 21, (3), pp. 91-95.
11. Belmans, R., Geysen, W., Jordan, H. and Vandenput, A. (1982): "Unbalanced magnetic pull in three-phase two-pole induction motors with eccentric rotor." IEE Conf. Publ. 213, 1982, pp. 65-69.
12. Wright, M. T., Gould, D. S. M. and Middlemiss, J. J. (1982): "The influence of unbalanced magnetic pull on the critical speed of flexible shaft induction machines," ibid., 1982, pp. 61-64.
13. Ellison, A. J. and Yang, S. J. (1971): "Effects of rotor eccentricity on acoustic noise from induction machines," Proc. IEE, 1971, 118, (1), pp. 174-184.
14. Erskine, J. B. (1978): "A users view of noise and vibration aspects of AC induction motors." IEE Colloquium Digest 1978, pp. 52-64.
15. Leonard, R. A. and Thomson, W. T. (1984): "Vibration and stray flux monitoring for unbalanced supply and interturn winding fault diagnosis in induction motors." Proceedings of 1st UK International Conference on Condition monitoring, University College of Swansea, Swansea, UK, April 1984, pp. 340-354.
16. Verma, S. P. and Natarajan, R. (1982): "Effects of eccentricity in induction motors." Proceedings of International Conference on Electrical machines, 3, Budapest, Hungary, Sept. 1982, pp. 930-933.
17. Binns, K. J. and Barnard, W. T. (1977): "Some aspects of the use of flux and vibration spectra in electrical machines." Proceedings of Conference on Applications on time-series analysis, University of Southampton, Southampton, UK, 1977, pp. 71.1-71.12.
18. Penman, J., Had wick, J. G. and Barker, B. (1978): "Detection of faults in electrical machines by examination of the axially directed fluxes." Proceedings of 3rd International Conference on Electrical machines, Brussels, Belgium, 1978, pp. R/5-1-R/5-1O.
19. Penman, J., Hadwick, J. G. and Stronach, A. F. (1980): "Protection strategy against the occurrence of faults in electrical machines." IEE Conf. Publ 185, 1980, pp. 54-58.
20. Thomson, W. T., Leonard, R. A., Deans, N. D. and Milne, A. J. (1983): "Condition monitoring of induction motors for availability assessment in offshore installations." Proceedings of 4th Euredata Conference, Venice, Italy, 1983.

21. Thomson, W. T., Leonard, R. A., Deans, N. D. and Milne, A. J. (1983): "Monitoring strategy for discriminating between different types of rotor defects in induction motors," 18th UPEC Proceedings, University of Surrey, Guildford, Surrey, UK, 1983, pp. 241-246.
22. Yang, S. J. (1981): "Low noise electric motors" (IEE Monographs in Electrical and Electronic Engineering, Oxford Science Publications, 1981).
23. Heller, B. and Jokl, A. L. (1969): "Tangential forces in squirrel cage induction motors," *IEEE, Trans*, 1969, PAS-88, (4), pp. 484-492.
24. Heller, B. and Hamata, V. (1977): "Harmonic field effects in induction machines" (Elsevier Scientific Publishing Company, 1977).
25. Carter, G. W. (1967): "The electromagnetic field in its engineering aspects" (Longmans, 1967).
26. Thomson, W. T., Leonard, R. A., Milne, A. J., and Penman, J. (1983): "Failure identification of offshore induction motor systems using online condition monitoring." Proceedings of 4th National Reliability Conference, Birmingham, UK, 1983, pp. 2C/3/1-2C/3/11.
27. Thomson W. T., Leonard, R. A., Deans, N. D. and Milne, A. J. (1983): "Condition Monitoring of induction motors for avalibility assement in offshore installations." in Proceedings of 4th Euredata Conference, Italy, 1983.
28. Thomson W. T., Leonard R. A., Deans N. D. and Milne A. J. (1983): "Monitoring strategy for discriminating between different types of rotor defects in induction motor," in 18th UPEC Proceedings, University of Surrey, UK, 1983.
29. "Monitoring strategy for discriminating between different types of rotor defects in induction motor," in 18th UPEC Proceedings, University of Surrey, UK, 1983.
30. Caneron, J. R., Thomson W. T. and Dow, A. B. (1986): "Vibration and Current Monitoring for detecting airgap eccentricity in large induction motors," IEE Proceedings, Vols. 133, Pt. B., no. 3, pp. 155-163, May 1986.
31. Chen, Shaotany, Zhong, Erkuan and Thomas, A. Lipo (1994): "A New Approach To Motor Condition Monitoring In Induction Motor Drives," *IEEE Transactions on Industry Applications*, vol. 30, no. 4, pp. 905-911, July/August 1994.
32. Nandi, Subhasis, Toliyat, Hamid A. and Li, Xiadong (2005): "Condition Monitoring and Fault Diagnosis of Electrical Motors – A Review." *IEEE Transactions on Energy Conversion*, Vol. 20, No.4, December 2005, pp. 719-729.
33. Khwaja, Hina A., Gupta, S. P. and Kumar, Vinod (2010): "A Statistical Approach for Fault Diagnosis in Electrical Machines." *IETE Journal of Research*, Vol. 56, Issue 3, May-June 2010, pp. 146-155.
34. Krikar K. S. and Numan Ali, H. (2007): "On-Line Current Based Condition Monitoring and Fault Diagnosis of Three - Phase Induction Motor," *Eng. & Technology*, Vol. 25, No. 3, 2007, pp. 395 - 406.
35. Mehala, Neelam and Dahiya, Ratna (2007): "Motor Current Signature Analysis and Its Applications in Induction Motor Fault Diagnosis," *Int. Journal of Systems Applications, Engineering & Development*, Vol. 2, 2007, pp. 29 - 35.
36. Singh, G. K. and Al Kazzaz, S. A. S. (2003): "Induction Machine Drive Condition Monitoring and Diagnostic Research a Survey," *Electrical Power System Res.*, 2003, 64(2), pp. 145 - 158.
37. Stavrou, A., Sedding, H. G. and Penman, J. (2001): "Current Monitoring for Detecting Inter-turn Short Circuit in Induction Motors," *IEEE Trans. Energy Convers*., 2001, 16, (1), pp. 32 - 37.
38. Tavner, P. J. (2008): "Review of Condition Monitoring of Rotating Electrical Machines," *IET Electric Power Applications*, 2008, Vol. 2, No. 4, pp. 215 - 247.
39. Trutt, F. C., Sottile, J. and Kohler J. L. (2002): "On-Line Condition Monitoring of Induction Motors," *IEEE Trans. Ind. Appl.*, 2002, 38 (6), pp. 1627 - 1632.
40. Tavner, Peter, Ran, Li, Penman, Jim and Howard, Sedding (2008): "Condition Monitoring of Rotating Electrical Machines," The Institution of Engineering and Technology, 2008.
41. Mitra, D. K. and Chatterjee, T. K. (1996): "A novel on-line condition monitoring instrumentation system for sheraer and AFC motors," *Journal of Mining Engineers*, UK, Jan 1996, Vol 78, no 783.
42. Chen, Shaotany, Zhong, Erkuan and Thomas, A. Lipo (1994): "A New Approach To Motor Condition Monitoring In Induction Motor Drives," *IEEE Transactions on Industry Applications*, Vol. 30, No. 4, July/August 1994 pp.905-911.
43. Nandi, Subhasis, Toliyat, Hamid A. and Li, Xiadong (2005): "Condition Monitoring and Fault Diagnosis of Electrical Motors – A Review." *IEEE Transactions on Energy Conversion*, Vol. 20, No.4, December 2005, pp. 719-729.
44. Kohler, J. L., Sottile, J. and Trutt, F. C. (2002): "Condition Monitoring of Stator Windings in Induction Motors: Part I-Experimental Investigation of the Effective Negative Sequence Impedance Detector." *IEEE Transacations on Industry Applications*, Vol. 38, No.5, Sep/Oct. 2002.
45. Kilman, G. B. and Stein, J. (1999): "Methods of motor current signature analysis." *Electr. Mach. And Power Sys.*, Vol. 5, No. 1, pp. 41-52, 1999.
46. Stout, David F. and Kaufman, Milton (1976): Handbook of Operational Amplifier Circuit Design, McGraw Hill, Inc, 1976.
47. Cameron, J. R. Thomson and Dow, A. B. (1986): "Vibration and curent monitoring for detecting airgap eccentricity in large induction motors." In IEE Proceedings, Vol. 133, Pt. B, No. 3, May 1986, pp 155-163.